Lab on a Chip

Dynamic Article Links

Cite this: *Lab Chip*, 2011, **11**, 1629

www.rsc.org/loc

PAPER

Optical tweezers directed one-bead one-sequence synthesis of oligonucleotides†

Tao Wang,*[a] Stefan Oehrlein,[b] Mark M. Somoza,‡[c] Jose R. Sanchez Perez,[b] Ryan Kershner[bd] and Franco Cerrina[bcef]

Received 9th November 2010, Accepted 14th March 2011
DOI: 10.1039/c0lc00577k

An optical tweezers directed parallel DNA oligonucleotide synthesis methodology is described in which controlled pore glass (CPG) beads act as solid substrates in a two-stream microfluidic reactor. The reactor contains two parallel sets of physical confinement features that retain beads in the reagent stream for synthetic reaction but allow the beads to be optically trapped and transferred between the reagent and the inert streams for sequence programming. As a demonstration, we synthesized oligonucleotides of target sequence 25-nt, one deletion and one substitution using dimethoxytrityl (DMT) nucleoside phosphoramidite chemistry. In detecting single-nucleotide mismatches, fluorescence *in situ* hybridization of the bead-conjugated probes showed high specificity and signal-to-noise ratios. These preliminary results suggest further possibilities of creating a novel type of versatile, sensitive and multifunctional reconfigurable one-bead one-compound (OBOC) bead array.

1 Introduction

Since its inception some fifteen years ago,[1] DNA microarray technology has promised to change the horizon of genomics and clinical medicine and recently entered the clinical prognostic and diagnostic arena for several types of cancer.[2,3] Although substantial efforts have been invested over the years in surface immobilization chemistries,[4] techniques to detect gene expression,[5] probe design optimization for mitigating cross-hybridization,[6] statistical algorithms for screening and genotyping[7] as well as vigorous comparative inter- and intra-platform studies,[8,9] the array platforms themselves have remained largely unchanged. There also has been little work to correlate the performance of microarrays with feature-wise DNA qualities, *e.g.* purity and amount.[10] The performance of such platforms may be fundamentally limited in part by the very nature of physics and chemistries in the microarray fabrication processes and the characteristics of probes. For DNA microarrays to serve as sensitive, robust detection or chip-based gene assembly platforms, it is imperative that DNA microarrays have synthetic or spotted oligonucleotide probes of high fidelity, high diversity and appropriate quantity. Unfortunately, no existing synthesis technology supports all three attributes concurrently and at a low cost.[11–13] Moreover, all existing microarrays are essentially in a static mode, where the biomolecules are patterned and immobilized at fixed locations on a 2D surface. A process-integrated, multifunctional concept, which can fully take advantage of microarrays' one-spot one-compound (OSOC) potential by combining combinatorial probe synthesis, immobilization, dynamic addressing and transportation of probes, hybridization, identification of positive hits, sorting and enrichment, as well as more sophisticated post-analysis needs, is out of reach of the current microarray paradigm.[14]

Oligonucleotides are synthesized base-by-base with a four-step cycling process consisting of deprotection, coupling, capping and oxidation on functionalized solid substrates using 5′-end protected nucleoside phosphoramidite monomers. *In situ* synthesis on 2D microarrays, directed by optical,[15–17] electrochemical,[18,19] photoelectrochemical[20] deprotection mechanisms or inkjet methods,[21–23] allow highly diversified oligonucleotide libraries of thousands of different sequences to be generated, but the quantity for each sequence is small, typically ~fmol.[17] In addition, because microarray fabrication is significantly more complex than single oligonucleotide synthesis, it is not surprising that their yield and purity are generally inferior. For example, in the widely used optically fabricated microarrays, the stepwise

[a]*Center for Nano Science and Technology, Department of Electrical Engineering, University of Notre Dame, Notre Dame, IN, 46556, USA. E-mail: twang5@nd.edu; Fax: +01 574 631 4393; Tel: +01 574 631 1353*
[b]*Materials Science Program, University of Wisconsin-Madison, Madison, WI, 53706, USA*
[c]*Center for Nanotechnology, University of Wisconsin-Madison, Madison, WI, 53706, USA*
[d]*Department of Mechanical Engineering, University of Wisconsin-Madison, Madison, WI, 53706, USA*
[e]*Department of Electrical and Computer Engineering, University of Wisconsin-Madison, Madison, WI, 53706, USA*
[f]*Department of Electrical and Computer Engineering, Boston University, Boston, MA, 02215, USA*

† This paper is dedicated to the memory of our colleague, mentor, and friend Professor Franco Cerrina, who tragically passed away during the preparation of this manuscript.

‡ Present address: Institute of Inorganic Chemistry, University of Vienna, Währinger Strasse, A-1090 Vienna, Austria.

coupling efficiencies are typically <98%,[24–27] resulting a purity <62% for 25-nt long probes. These factors combined make it difficult for microarrays to reliably measure gene expressions, and the results are often arguably not reproducible from one platform to another.[9,10,28] In contrast, the conventional approaches using controlled pore glass (CPG) bead packed columns or wells and solid-phase dimethoxytrityl (DMT) phosphoramidite chemistry offer oligonucleotides of high fidelity (stepwise coupling efficiency >99%),[29–31] but the sequence output is limited to one sequence per column, and the synthetic scales are often excessive.

Recently, microfluidic approaches have emerged for DNA oligonucleotide synthesis. The representative approaches include the synthesis on collective CPG beads in an elastomer perfluoropolyether (PFPE) synthesizer developed by Quake and coworkers,[32,33] Si/parylene hybrid microchannel reactor in the Gao and Guluri groups[34] and polydimethylsiloxane (PDMS) microreactor by Southern *et al.*[35] This microfluidic method not only inherits the highest stepwise efficiency (99.5%)[34] from the column approaches, but also consumes much less reagent (60-fold reduction).[32] Nevertheless, the generation of diverse sequence libraries on a one-bead one-compound (OBOC) fashion,[36–39] similar to OSOC, remains a critical challenge. Such OBOC libraries are much more appealing than the conventional microarray because they offer enormous potential for technological breakthroughs in single bead based dynamically reconfigurable, flexible, sensitive and multifunctional high-throughput biomolecule manipulation and detection systems on a single integrated chip. Towards this end, Takeuchi's group[14] recently designed a multifunctional bead microarray to dynamically immobilize and transfer particles, infuse reagents, monitor reaction, and retrieve interested particles on a single chip using hydrodynamic confinement and optical-based microbubbles. However, due to great challenges faced in seeking effective, combinatorial single bead manipulation tools and suitable systems, this emerging research area still remains in its early infancy.

In this paper, we report a proof-of-principle, CPG bead-based microfluidic methodology capable of performing multiple functions, *e.g.* synthesis of programmed oligonucleotide probes from DMT phosphoramidite chemistry using optical tweezers,[40,41] reconfigurable bead manipulation, *in situ* hybridization and optical fluorescence detection, all on a single chip. To the best of our knowledge, this is the first demonstration of optical tweezers directed combinatorial DNA synthesis with the ability to construct oligonucleotides in a precisely controlled one-bead one-sequence mode on a single desired CPG bead. As a microfluidic-compatible manipulation tool, optical trapping provides significant advantages, including non-contact, rapidly reconfigurable actuation for applications ranging from sorting[42] to assembly.[43] These features allow us not only to externally manipulate the beads inside the channel without significantly modifying the microfluidic device itself, but also to open up further possibilities of creating a novel type of versatile, sensitive and multifunctional reconfigurable OBOC bead array on the very same single chip. Moreover, it is feasible to both scale up the diversity by incorporating multiple reactors in a single chip and achieve equivalent total synthesis times as in the production of conventional arrays (*i.e.* optical, electrochemical and inkjet printing) by implementing well-established, autonomous and automatic computer-controlled high-resolution, high-throughput algorithm, programming and synchronization in the optical manipulation system. Furthermore, the adoption of nanoporous beads further enhances the synthesis and hybridization kinetics and therefore the performance of the bead microarray.[44] We show conceptual design, microreactor fabrication, parallel synthesis, detection of single-nucleotide mismatches, and comparison with the standard synthesis in columns.

2 Proof-of-principle design

2.1 Parallel synthesis strategy

The principle for achieving parallel synthesis on CPG beads in a two-stream laminar flow microchannel is illustrated in Fig. 1. All reagents for synthetic reaction steps, *i.e.* deprotection, coupling, capping, oxidation and washing are sequentially pumped through one stream (called reagent stream) from the left to the right. The inert chemical, *i.e.* acetonitrile, is run through the other stream (called inert stream) in the same direction. The liquid/liquid interface between these two streams can be well-maintained with little mixing by running these two streams side-by-side at the same velocity. All derivatized beads are initially held in the confinement features in the inert stream. Then the selected beads are captured and transferred using optical tweezers to the corresponding confinement features in the reaction stream, where the 5′-DMT is chemically removed and the first nucleotide is coupled. The coupled beads are then capped, oxidized, washed in the reaction stream with sequentially pumped-in reagents and moved back to the inert stream. In the

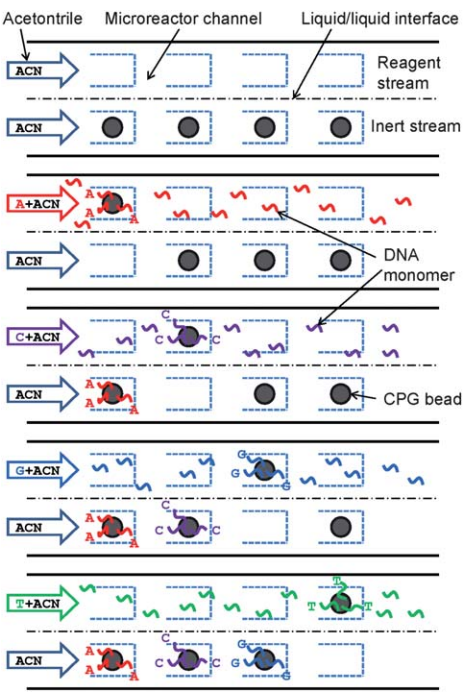

Fig. 1 Schematic of parallel synthesis cycles to achieve different DNA oligomers by temporal and spatial manipulation of CPG beads in a two-stream microchannel.

second cycle, the next selected phosphoramidite flows in after the deprotection step, and a similar manipulation is performed to another batch of selected beads to add the nucleotide of cytosine. Each transfer cycle adds one nucleotide to the growing oligomer chain. Such an operation is repeated until the desired sequences and lengths are accomplished on each CPG bead of interest, resulting in a multiplexed unique sequence on each bead.

2.2 Microreactor configuration

To better illustrate the optical tweezers directed parallel synthesis, a simplified microreactor configuration with a straight channel and open-end bead confinement features is shown schematically in Fig. 2. The actual layout used for the experiment that includes side loading channels and more complicated confinements having side openings for bead transport will be described in the Experimental section. The patterned top polydimethylsiloxane (PDMS) thick layer has four fluidic ports: two inlets at the Y-shaped ends for reagent and inert chemical delivery and two outlets at the T-shaped ends for waste drainage. The microfluidic reactor is constructed by bonding this PDMS channel layer to a 170 μm thick coverglass slide, through which the laser beam is transmitted upwards to trap and manipulate beads inside the channel. Such a thin coverglass is chosen to ensure that the laser focal point falls inside the channel, effectively trapping beads even with a 100× objective lens (oil immersion, NA = 1.4).

The reactor channel consists of two parallel sets of physical features that permit beads to be moved in and out with optical actuation, but to be confined in place for oligomer synthesis during which the optical trapping is absent. With the use of a fenced confinement layout for the confinement, the beads are confined inside the features against possible fluid perturbation during the synthesis process. By optically trapping and transferring as well as physically confining, the selected beads are either exposed to the reagent stream or stored in the chemically inert stream so that programmed sequences can be grown on the beads of interest. Side channels (not shown here) are used to facilitate bead loading. The main channel is 1.5 mm wide to mitigate the liquid/liquid interfacial mixing. The internal geometry of the reaction cell is defined by 100 μm thick channel patterns. Given the straight channel length 1.67 cm, the total inside volume of the reactor is approximately 2.5 μl, which is 2 orders of magnitude smaller than a typical synthetic column. Such a wide channel also ensures effective optical trapping because the laser beam waist is typically less than ~3 μm.

2.3 Synthetic scale on CPG beads

The synthetic scales on single CPG beads are estimated based on the specific area, pore size, bead size and bulk density of SiliaSphere silica beads provided by the vendor Silicycle (Quebec, Canada). Fig. 3 shows the synthetic scales calculated from the vendor data as well as scanning electron micrograph and optical image of the CPG beads utilized in this work (nominal 20~45 μm diameter with 1000 Å pores and density 0.486 g cm^{-3}). The surface density of the oligonucleotide to be synthesized is estimated to be 100 pmol cm^{-2}.[45] It is expected that the amount of oligonucleotide on one single bead is ~1 pmol, as highlighted in the figure. In contrast to a typical ~fmol product yield of a single feature on a microarray,[17] this represents an increased capacity of 2~3 orders of magnitude.

2.4 Two-stream laminar flow interface

One crucial requirement for successful parallel synthesis in the laminar flow channel is to keep the two streams, *i.e.* reagent stream and inert chemical stream, separated to such an extent that the CPG beads downstream are not exposed to the unwanted stream. In a pressure-driven two-stream flow through a rectangular-shaped cross-sectional channel with a relatively

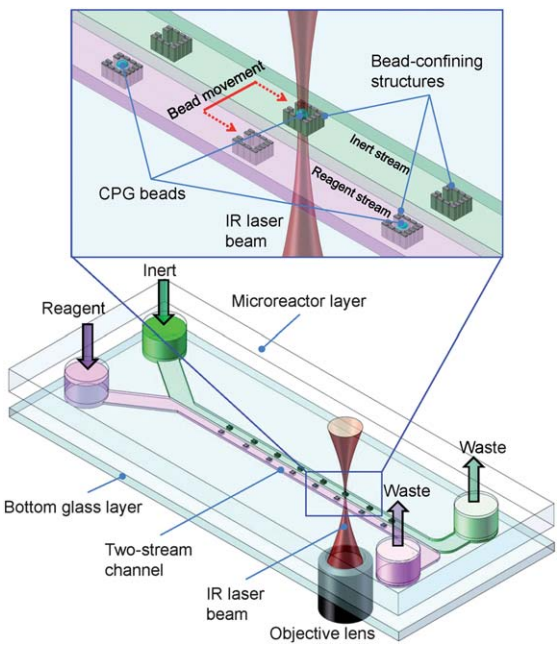

Fig. 2 Schematic configuration of the optical tweezers directed two-stream laminar flow synthesizer with simplified straight channel and open-end bead confinement features. The top close-up shows details of two streams, trapping laser beam, confinement features, CPG beads and bead transfer route. See Experimental section for the actual chip layout.

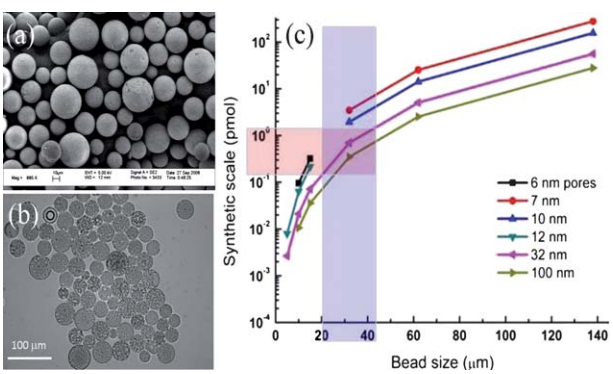

Fig. 3 CPG beads and estimated synthetic scales: a scanning electron micrograph (a) and an optical image (b) of 20–45 μm diameter beads with 1000 Å pores as well as synthetic scales of single CPG beads with varied pore and bead sizes (c). The quantity of oligonucleotide one 20–45 μm diameter bead yields is highlighted, ~1 pmol.

large aspect ratio (channel width over channel height), the diffusion length or mixing width can be approximated as

$$\delta = \sqrt{2DL/v} \quad (1)$$

where δ is the width of the mixing region across the channel, D diffusion coefficient, L channel length and v fluid velocity.

Fig. 4 shows the estimated mixing widths at the end of the channel as a function of flow velocities. The figure includes both water and acetonitrile for two channel lengths 1.0 cm and 1.67 cm, respectively. The inset shows the relationship between average velocity and volumetric flow rate for three rectangular cross sections. For a typical flow rate 100 μl min^{-1} in a channel with a cross section 100 μm × 1000 μm and 1.67 cm in length, the mixing width is <5 μm. This can be well tolerated by using a wider channel, *e.g.* ~1.5 mm, and larger spacing between two corresponding confinement features.

2.5 Optical manipulation of CPG beads

To effectively manipulate CPG beads, the optical trapping forces generated by optical tweezers have to be greater than drag forces that the beads experience in the fluid. In most microfluidic environments, the Reynolds number (Re) is <1 and the viscous drag force F_d generated by a flowing fluid on a *nonporous* spherical bead can be calculated from a modified Stokes' equation:[48]

$$F_d = \frac{6\pi\eta r v}{1 - 1.004\left(\frac{r}{l}\right) + 0.418\left(\frac{r}{l}\right)^3 + 0.21\left(\frac{r}{l}\right)^4 - 0.169\left(\frac{r}{l}\right)^5} \quad (2)$$

where η is dynamic viscosity, r is the radius of the bead, v is the velocity of the bead and l is the half height of the flow cell or microchannel. At equilibrium, the optical trapping force on the bead is balanced with the drag force so that the trapping force can be calculated. For the case where the channel height is 100 μm and acetonitrile (η = 3.5 × 10^{-4} Pa s) is the medium, the

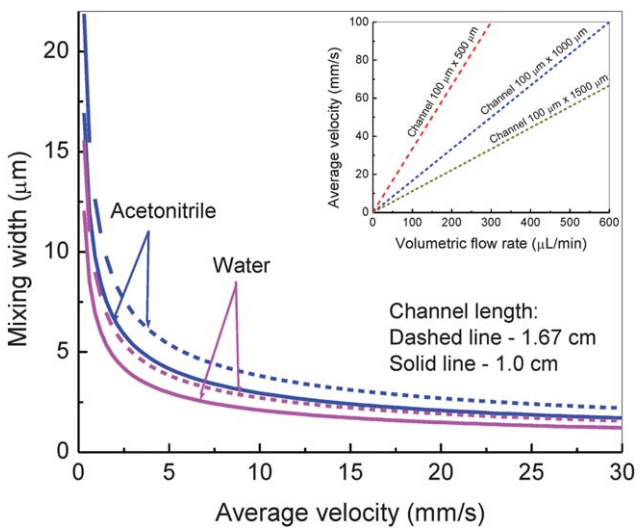

Fig. 4 Estimated mixing widths of water and acetonitrile at an end of channel using the 1-D diffusion model. The diffusion coefficients used are 2.2 × 10^{-9} m^2 s^{-1} for water[46] and 4.34 × 10^{-9} m^2 s^{-1} for acetonitrile.[47]

solid beads equivalent to the CPG beads used in this work (nominal 20–45 μm diameter with 1000 Å pores) will experience a drag force F_d 16.5~50.1 pN at v = 100 μm s^{-1}, 82.5~250 pN at v = 500 μm s^{-1}, and 165~501 pN at v = 1000 μm s^{-1}. The trapping force of a strongly focused laser beam can be as large as 300 pN,[49] therefore insufficient trapping could occur as v becomes greater than a certain value. In this scenario, the bead transfer can be executed in the presence of only inert acetonitrile at a lower or zero velocity. For *porous* beads, the actual drag force is smaller due to their high permeability to fluid flow.[50] Characterization of the interaction between the optical trap and porous beads as well as optical manipulation of the beads in the channel reactor will be reported elsewhere.[51]

3 Experimental

3.1 Reagents

For the synthesis experiments, the following reagents were purchased from Glen Research (Sterling, VA): 5′-Dimethoxytrityl-*N*-benzoyl-2′-deoxyadenosine 3′-[(2-cyanoethyl)- (*N*,*N*-diisopropyl)-phosphoramidite (dA-CE Phosphoramidite), 5′-Dimethoxytrityl-*N*-benzoyl-2′-deoxycytidine 3′-[(2-cyanoethyl)-(*N*,*N*-diisopropyl)]-phosphoramidite (dC-CE Phosphoramidite), 5′-Dimethoxytrityl- N-isobutyryl-2′-deoxyguanosine 3′-[(2-cyanoethyl)-(*N*,*N*-diisopropyl)]-phosphoramidite (dG-CE Phosphoramidite), 5-Dimethoxytrityl-2′-deoxythymidine 3′-[(2-cyanoethyl)-(*N*,*N*-diisopropyl)]-phosphoramidite (dT-CE Phosphoramidite), activator 5-Ethylthio-1*H*-tetrazole (0.25 M solution in anhydrous acetonitrile), capping reagents Cap Mix A tetrahydrofuran (THF)/acetic anhydride (Ac_2O) (9 : 1) and Cap Mix B 10% N-Methylimidazole (MeIm) in THF/pyridine (8 : 1). The following reagents were purchased from Aldrich (Milwaukee, WI): iodine (purity >99.99% trace metals basis), pyridine (anhydrous, purity 99.8%), acetic acid (ACS reagent, purity >99.7%), trifluoroacetic acid (TFA, ReagentPlus, purity 99%), dry acetonitrile (purity >99.5%, <30 ppm water) and anhydrous acetonitrile (purity >99.8%, <10 ppm water). For hybridization experiments, 25-nt 5′-end Cy3 labelled complementary oligonucleotide 5′-/5Cy3/GAC CAG GGT GGT TCA TGA TGA TGA C -3′were purchased from IDT (Coralville, IA). All reagents were used without further purification.

3.2 Fabrication of microfluidic reactors

The microfluidic reactors were fabricated using soft lithography.[52] The reactor patterns were generated on a 5″ × 5″ chrome mask. A 4″ Si wafer was first cleaned using the Piranha procedure. A layer of 100 μm thick SU-8 2100 layer was spun on the wafer at 3000 rpm for 30 s following a spread of resist at 500 rpm for 8 s. The coated wafer was then soft baked on a hot plate at 65 °C for 5 min followed by baking on a second hot plate at 95 °C for 25 min. The SU-8 was exposed with the chrome mask at 260 mJ cm^{-2} at 365 nm on a Karl Suss MA6/BA6 contact aligner. The wafer was then post-baked on a hot plate at 65 °C for 5 min followed by baking on another hot plate at 95 °C for 12 min. The SU-8 was then developed in SU-8 developer poly (ethylene-*co*-glycidyl methacrylate) (PGEMA) with agitation for 12–14 min to complete the SU-8/Si master fabrication.

The PDMS structure layer was cast with the SU-8/Si master. 184 Sylgard Elastomer monomer and curing agent (Dow Corning) were first mixed at a 10 : 1 ratio by weight. The mixture was poured onto the SU-8/Si master placed in a plexiglass petri dish and degassed in a desiccator under vacuum until air bubbles were removed. After this, the PDMS was baked on a hot plate at 85 °C for 2 h. Prior to plasma assisted bonding, the coverglass slip was cleaned in an ultrasonic bath followed by the Piranha and then dried with N_2. The cured PDMS layer was peeled from the SU-8/Si master immediately before bonding, cut to lithographically predefined size and punched to form connect-through holes using a flat head needle. Both the PDMS piece and coverglass slip were plasma oxidized in a plasma cleaner (Harrick). Next, the two pieces were brought into contact and any air bubbles were removed with a slight pressure. The assembly was then baked on a hot plate at 135 °C for 10 min. This resulted in an irreversible bond at the PDMS/glass interface. Finally, polytetrafluoroethylene (PTFE) tubing leads with OD/ID 0.06″/0.02″ were inserted into the inlet and outlet holes to complete the device. Fig. 5 shows a completed PDMS/glass microfluidic synthesizer with the actual side loading channels and confinements having side openings.

3.3 Silanization of CPG beads

Hybridization kinetics are known to be improved by linkers which distance the DNA probe sequence from the substrate surface.[53] DNA microarray subtracts are typically functionalized with silane linker molecules that also provide free hydroxyl groups for initiating oligonucleotide synthesis. This procedure was modified and applied to the CPG beads in this work. First, 1000 ml 95% EtOH Stock Solution (950 ml EtOH and 50 ml MilliQ water, >18 M Ω-cm) was mixed and 1 ml glacial acetic acid was added to adjust pH to 4–5. Next, 400 ml 2% silane solution was prepared by adding 8 ml silane N-(3-triethoxysilylpropyl)-4-hydroxybutryamide ($C_{13}H_{29}NO_5Si$, Gelest, Inc., Morrisville, PA) to a 392 ml stock solution. The pure silica CPG beads were first soaked in a vial with the silane solution to form a suspension and then agitated with a rotating agitator for 4 h with mild rotation. Then the vial was centrifuged at 3000 rpm, and the silane solution was decanted. The beads were then washed 5 times for 5 min each in 95% EtOH in a centrifugal concentrator at the same rotation speed and decanted each time. The final bead slurry was then drawn with a pipette and spread on a flat glass plate followed by a cure at 120 °C for 1 h in an oven, and then vacuum cured at the same temperature overnight.

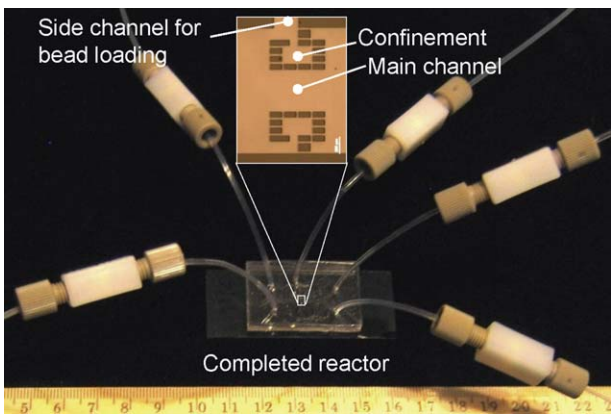

Fig. 5 A completed PDMS/glass microfluidic synthesizer with the actual side loading channels and confinements having side openings with PTFE tubings and microfluidic connectors. The inset is an optical micrograph showing a pair of confinement features inside the reactor channel.

3.4 Optical tweezers setup

The optical tweezers system was constructed on a vibration isolation table, as shown in the top panel of Fig. 6. The laser light source was a YLR-10-1064-LP ytterbium fiber laser (IPG Photonics, Oxford, MA) that provides a continuous wave TEM_{00} mode at a maximum power of 10 W in a linearly polarized, single-transverse-mode beam at 1064 nm with 1 nm linewidth. The infrared 1064 nm wavelength was chosen because it could be separated from the imaging light and also minimized the possible damage to biological materials caused by light absorption and scattering. The laser beam was directed into a quartz half-wave plate and then into a polarizing cube beam splitter. After the beam splitter, the light beam was expanded 2× with the first telescope. The second 1 : 1 telescope provided the final beam and images the plane of the steerable mirror onto the back focal plane of an objective lens. The laser light was finally directed into the back aperture of an objective lens mounted on an inverted microscope (1X71, Olympus). After expansion, the beam size became approximately 10.6 mm in diameter, overfilling the 9.0 mm back aperture of 20× objective (NA = 0.5) and 7.2 mm back aperture of 60× water-immersion objective (NA = 1.2). A single microscope objective was used for both laser trapping and image acquisition. A customized LabVIEW interface was used to dynamically control the optical tweezers. A software (Prior ProScan II) was used to control the movement of the motorized stage. Trapping images and video clips were recorded with

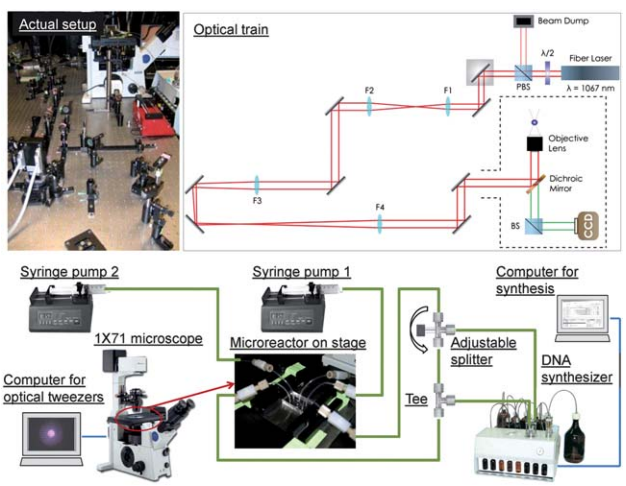

Fig. 6 Parallel synthesis experiment setup. Top panel: photo and schematic of the optical setup showing expansion of linearly polarized fiber laser using lenses F1 ($f = 100$ mm) and F2 ($f = 200$ mm); a second telescope (lenses F3 and F4, $f = 500$ mm) produces a conjugate plane at the back aperture of the microscope objective. The dashed-lined part is the location of the microscope. Bottom panel: schematic of synthesis systems showing microreactor on microscope, reagent delivery and control computers for optical trapping and synthesis.

a Lumenera Infinity 2 (Ottawa, Canada) digital microscope camera and Infinity Capture software.

3.5 Optical tweezers directed oligonucleotide synthesis

The complete parallel synthesis setup that includes optical tweezers, microreactor, fluid delivery and control is schematically shown in Fig. 6. To test the parallel synthesis, the experiment was designed to include the target 25-nt oligomer with sequence 5′-GTC TAC ATC ATG AAC CAC CCT GGT C-3′, a sequence with one deletion 5′-GTC TAC ATC ATG AA_ CAC CCT GGT C-3′, another sequence with one substitution 5′-GTC TAC ATC ATG AAT CAC CCT GGT C-3′ and a control group. For each oligonucleotide, 5 "T "s were first coupled to the silanized beads to act as a molecular linker. The detailed operation steps are illustrated in Fig. 7. Two streams were run through the reactor. One stream ran exclusively with synthesis reagents from an Azco Oligo-800 DNA/RNA synthesizer (Azco Biotech, San Diego, CA), while the other stream, with pure acetonitrile, flowed from a syringe pump at a flow rate of 200 μL min^{-1}. The beads were actuated as needed to produce the desired sequences using an incident laser power ~0.8 W with a 20× microscope objective.

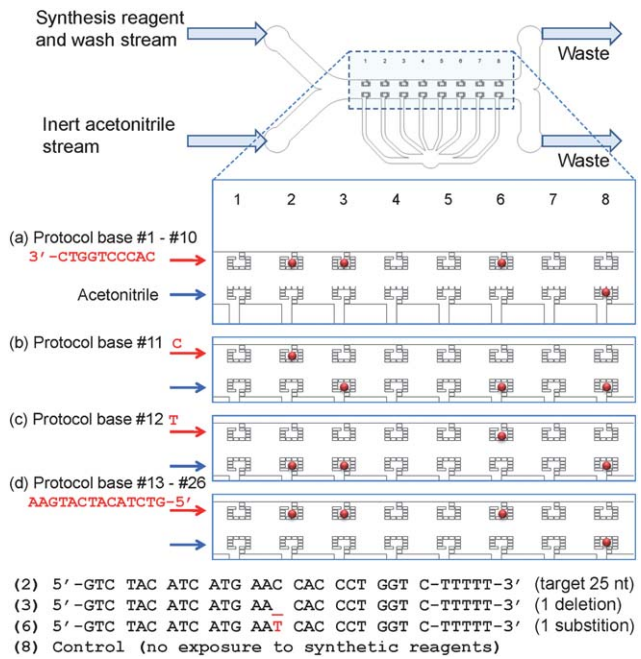

Fig. 7 Sequences and illustrative protocol of optical tweezers directed parallel synthesis operation in the actual two-stream microreactor. The top stream runs exclusively with synthesis reagents and washing buffers while the bottom stream runs with inert acetonitrile. The number in front of the sequences indicates bead positions inside the channel. (a) The synthesis cycles were run until bases 1 to 10 from the protocol were added. (b) The beads 3 and 6 were optically moved back to the inert stream. Base C was only added to bead 2 when the coupling reagents ran through the upper stream. (c) Beads 2 and 6 were moved into the opposite features, and base T was added to bead 6. (d) Beads 2 and 3 were then moved to the reagent stream. The synthesis was continued by adding protocol bases 13 to 26 to complete the synthesis. Throughout the process, the beads inside the lower feature 8 were kept in place as a negative control without exposure to the synthetic reagents. Finally, all the beads were hybridized *in situ* following the procedure described in section 3.6.

In the synthesis protocol, we adopted the recipe for deprotection and oxidation steps from Southern's group.[35] For deprotection, 10% (w/w) aqueous trifluoroacetic acid (TFA) was run for 2 min. Following deprotection, phosphoramidites (0.05 M in acetonitrile) were coupled in 0.45 M tetrazole in acetonitrile for 1 min. For capping, tetrahydrofuran (THF)/acetic anhydride (Ac_2O) (9 : 1) and 10% N-Methylimidazole (MeIm) in THF/pyridine (8 : 1) were run alternatively with a total time 2 min. For oxidation, 0.1 M iodine in 9 : 1 pyridine/acetic acid (v/v) was run for 1 min after the synthesis was complete. Beads were washed within acetonitrile stream for 1 min after each step.

In a series of parallel experiments, oligonucleotides were also synthesized in customized columns containing the silanized CPG beads for verifying the identical synthesis sequences and protocol using the same chemistry. This was then used as a benchmark for comparison with the synthesis results obtained from the microreactor.

3.6 Cy3-labelled hybridization

After completing the synthesis, the beads were left in the column or reactor with the tubing connected. A solution of ethylenediamine-ethanol (1 : 1) was injected for 2 h with a syringe to remove the base protecting groups. The hybridization solution (Cy3-labelled probes, 100 nM 60 μl, 2× MES hybridization buffer 300 μL, nuclease-free water 240 μL, total 600 μL) was heated to 95 °C for 5 min in a heat block and then incubated at 45 °C for 5 min. The 2× MES hybridization buffer was made from 100 nM MES, 1 M [Na+], 20 mM EDTA and 0.01% Tween 20. The CPG beads were then hybridized with this hybridization solution delivered by a syringe for 2 h. The CPG beads were washed using Nimblegen Wash Buffer protocol (Roche-Nimblegen) with syringe delivery. The beads were then examined with the fluorescence microscope equipped with a broadband light source (EXFO 2000, Quebec, Canada) and with a XF115-2 filter set (Omega Optical, Brattleboro, VT). All the fluorescence images were taken using an Infinity CCD camera with Infinity Capture software (Lumenera Corporation, Ottawa, Ontario Canada) under the same conditions.

4 Results and discussion

4.1 One-bead one-sequence capability

Cy3 fluorescence images and raw intensities (acquired using ImageJ software) of parallel synthesis results from the microreactor with the sequences and control outlined in 3.5 are shown in Fig. 8. The intensity levels indicate that the 25-nt target sequence is readily discriminated from one substitution or one deletion oligonucleotides, although the difference between the latter two is marginal. The negative control showed only weak fluorescence associated with the silanized CPG beads. As a benchmark, Fig. 9 shows the Cy3 fluorescence images and raw intensities of hybridized identical DNA oligonucleotides synthesized in our custom-made CPG packed columns. The similar trend of the fluorescence intensities on the individual beads can be readily observed, that is, the target 25-nt sequence shows the strongest intensity with the significantly decreased intensity on one substitution, one deletion and the negative control beads.

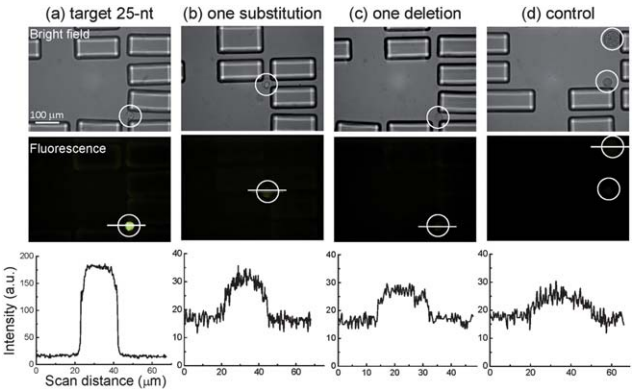

Fig. 8 Hybridized Cy3 fluorescence images of the synthesized oligomers on CPG beads in optical tweezers directed microreactor synthesizer. The sequences are outlined in Fig. 7: 25-nt target (a), one substitution (b), one deletion (c) and negative control (d). Top panel: bright field, middle panel: fluorescence, and bottom panel: raw fluorescence intensities.

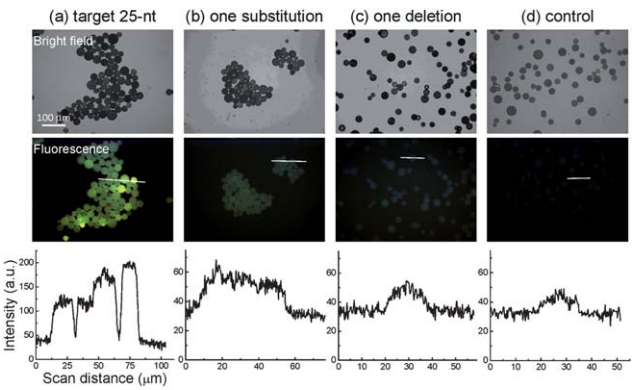

Fig. 9 Hybridized Cy3 fluorescence images of the synthesized oligomers on CPG beads in CPG bead packed column synthesizers. The sequences are the same as specified in Fig. 7: 25-nt target (a), one substitution (b), one deletion (c) and negative control (d). Top panel: bright field, middle panel: fluorescence, and bottom panel: raw fluorescence intensities.

These two sets of the fluorescence images were qualitatively analyzed with ImageJ. The fluorescence intensities of the oligomers were acquired from linescans across the beads (Fig. 8 and 9) and normalized to the mean fluorescence intensity of 25-nt target beads in each platform. The background fluorescence intensities were obtained by averaging the intensities of areas on the images that contain neither CPG beads nor PDMS confinement features. Fig. 10(a) shows normalized fluorescence intensities of the CPG beads for both cases. In either case, the target oligomers had fluorescence intensities at least 2.5 times as great as those of the one-substitution and one-deletion sequences. The intensity of the one substitution oligomers were slightly higher than those of the one-deletion oligomers, and the intensity of the one-deletion oligomers were about the same as that of the control group. Fig. 10(b) shows signal-to-noise (S/N) ratios of the fluorescence intensities for both cases. The S/N ratios were estimated using

$$S/N = \frac{I_f - I_{bg}}{SD_{bg}} \quad (3)$$

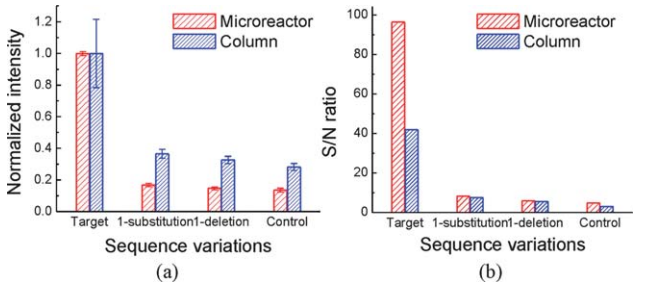

Fig. 10 Comparison of fluorescence intensities of oligonucleotides with target 25-nt, one substitution, one deletion and control on CPG beads prepared in columns and microreactor: normalized intensities (a) and S/N ratios (b).

where I_f is typical fluorescence intensity on bead, I_{bg} average fluorescence intensity on background, and SD_{bg} the standard deviation of background intensity. It can be seen that the S/N ratio of the target oligomer in either case was above 42, while the ratios of all other beads were less than 8. This presents a 4-fold difference between the target and one-substitution oligomers. While the differences between the one-substitution, one deletion oligomers were relatively small, the much higher intensities and S/N ratios of the target sequences indicated that the bead-conjugated probes were very suitable for single base discrimination assays. Although the fluorescence intensity levels and S/N ratios from the beads prepared in the microreactor were different from their counterparts in the column, presumably due to non-stringently controlled reagent batches, the overall trends remained similar. Therefore, the parallel synthesis results using the optical tweezers/microfluidic approach were comparable to those produced in the well-established CPG bead packed columns. These preliminary results clearly indicate that this integrated approach is capable of directing multiplex DNA syntheses and generating unique oligonucleotide sequence libraries in an one-bead one-sequence fashion.

4.2 Potential applications

In most circumstances, affinity-based bioassay and diagnostics require execution of a series of procedures ranging, for example, from probe synthesis, immobilization, pre-concentration, sorting, binding reaction to detection as well as multiple washing steps. Thus the ability to *in situ* construct probes from scratch, locate, trap and transfer the bead-conjugated probes to required locations at will inside a microfluidic platform is necessary in advanced integrated lab-on-a-chip systems.[14,54,55] Our prototype system, as demonstrated here, not only synthesizes probes on the carrier beads *in situ* and in parallel, but also serves as an *in situ* hybridization and detection platform. Moreover, the beads are physically addressable and dynamically reconfigurable, enabling novel functionalities, such as sorting, enrichment, capture and release, to execute more sophisticated post-analysis needs which are out of reach of the current array paradigm.

Although the number of oligonucleotides demonstrated here is limited, this work represents the early development toward a potentially powerful array principle. We envision that the scaled-up parallel strategy allows for creating novel reconfigurable, sensitive and multifunctional "mobile" DNA arrays

for demanding lab-on-a-chip biological and biomedical applications, *e.g.* microfluidic gene assembly,[56,57] low-abundance single-nucleotide polymorphism (SNP) genotyping,[58] bead-conjugated molecular libraries[36,38,39] and novel prognostic and diagnostic biosensors.[28] For example, by combining this approach with microfluidic-based gene assembly[56,57] it is feasible to create a "true gene chip" technology, which directly produces genes with lengths of several hundred or several thousand bases on a single chip from scratch and without polymerase chain reaction (PCR) amplification. The ability to produce small volumes of short oligonucleotides on-demand may also find broad application to DNA nanostructures, where a wide range of custom-tailored sequences are particularly useful for producing ever more complex architectures.[59] Furthermore, a fast, high-throughput microfluidic assay, *e.g.* immunoassay involving multi-stream binding and washing steps,[54,55] can also be designed. Although this approach is exemplified through oligonucleotide synthesis, it can be considered as a universal solid-phase process that may be extended to other biochemical and biological systems for building other OBOC libraries, such as peptides and oligosaccharides.

Finally, it is beneficial to take into account the synergetic outcomes of integrating our approach with the BeadArray format developed by Illumina,[60] which is based on etched bundles of fused optical fibers. The BeadArray consists of the array of micro-sized beads assembled in the etched micro-wells at high density. For nucleic acid assay, silica or polystyrene beads are first attached with *ex-situ* synthesized ssDNA probes, randomly loaded onto the micro-well array and then decoded with tedious multiple protocols to identify their specificities.[61] However, the system developed in this work *in situ* fabricates bead-conjugated probes in known locations and therefore no decoding procedure is required.

5 Conclusions

We have developed a methodology that allows synthesizing different oligonucleotides with desired sequences in parallel on CPG beads in a one-bead one-sequence fashion. The microfluidic reactor contains two parallel sets of physical confinement features that retain beads in the reagent stream for synthetic reaction but allow the beads to be optically trapped and transferred between the reagent and the inert streams for sequence programming. Using DMT nucleoside phosphoramidite chemistry, we have demonstrated the initial parallel synthesis of several different oligonucleotides, including the target 25-nt, one deletion and one substitution, in a single synthetic run. Hybridization with fluorescently labelled complementary ssDNA indicated that these products were comparable to their counterparts synthesized in CPG bead packed columns. These probes also showed high hybridization specificity as evidenced by a significant signal-to-noise ratio in detecting single-nucleotide mismatches. With judicious modifications and a scale-up, it is feasible to create a novel type of versatile, sensitive and multi-functional reconfigurable OBOC bead array that can be useful for many new and improved bead-based lab-on-a-chip applications.

6 Acknowledgements

This project was funded in part by the National Institutes of Health (NIH) under R01 HG003275 (to FC) and the Center for Nanotechnology at the University of Wisconsin – Madison.

References

1 M. Schena, D. Shalon, R. Davis and P. Brown, *Science*, 1995, **270**, 467–470.
2 X. Li, R. J. Quigg, J. Zhou, W. Gu, P. N. Rao and E. F. Reed, *Current Genomics*, 2008, **9**, 466–474.
3 Y. Shen and B.-L. Wui, *Clin. Chem.*, 2009, **55**, 659–669.
4 C. Heise and F. Bier, *Immobilisation of DNA on Chips II*, 2005, vol. 261, pp. 1–25.
5 V. K. Khanna, *Biotechnol. Adv.*, 2007, **25**, 85–98.
6 K. L. Gunderson, F. J. Steemers, G. Lee, L. G. Mendoza and M. S. Chee, *Nat. Genet.*, 2005, 549–554.
7 X. Di, H. Matsuzaki, T. A. Webster, E. Hubbell, G. Liu, S. Dong, D. Bartell, J. Huang, R. Chiles, G. Yang, M.-m. Shen, D. Kulp, G. C. Kennedy, R. Mei, K. W. Jones and S. Cawley, *Bioinformatics*, 2005, **21**, 1958–1963.
8 MAQC-Consortium, *Nat. Biotechnol.*, 2006, **24**, 1151–1161.
9 P. Tan, T. Downey, E. Spitznagel, P. Xu, D. Fu, D. Dimitrov, R. Lempicki, B. Raaka and M. Cam, *Nucleic Acids Res.*, 2003, **31**, 5676–5684.
10 S. Draghici, P. Khatri, A. Eklund and Z. Szallasi, *Trends Genet.*, 2006, **22**, 101–109.
11 M. J. Czar, J. C. Anderson, J. S. Bader and J. Peccoud, *Trends Biotechnol.*, 2009, **27**, 63–72.
12 D. J. Mueller, J. Helenius, D. Alsteens and Y. F. Dufrene, *Nat. Chem. Biol.*, 2009, **5**, 383–390.
13 J. Tian, K. Ma and I. Saaem, *Mol. BioSyst.*, 2009, **5**, 714–722.
14 W.-H. Tan and S. Takeuchi, *Proc. Natl. Acad. Sci. U. S. A.*, 2007, **104**, 1146–1151.
15 R. J. Lipshutz, S. P. A. Fodor, T. R. Gingeras and D. J. Lockhart, *Nat. Genet.*, 1999, **21**, 20–24.
16 S. Singh-Gasson, R. D. Green, Y. J. Yue, C. Nelson, F. Blattner, M. R. Sussman and F. Cerrina, *Nat. Biotechnol.*, 1999, **17**, 974–978.
17 J. Tian, H. Gong, N. Sheng, X. Zhou, E. Gulari, X. Gao and G. Church, *Nature*, 2004, **432**, 1050–1054.
18 R. D. Egeland and E. M. Southern, *Nucleic Acids Res.*, 2005, **33**, e125.
19 M. Maurer, C. Cooper, M. Caraballo, J. Crye, D. Suciu, A. Ghindilis, J. A. Leonetti, W. Wang, F. M. Rossi, A. G. Stver, C. Larson, H. Gao, K. Dill and A. McShea, *PLoS One*, 2006, **1**, e34.
20 B. Y. Chow, C. J. Emig and J. M. Jacobson, *Proc. Natl. Acad. Sci. U. S. A.*, 2009, **106**, 15219–15224.
21 E. M. LeProust, B. J. Peck, K. Spirin, H. B. McCuen, B. Moore, E. Namsaraev and M. H. Caruthers, *Nucleic Acids Res.*, 2010, **38**, 2522–2540.
22 A. P. Blanchard, R. J. Kaiser and L. E. Hood, *Biosens. Bioelectron.*, 1996, **11**, 687–690.
23 T. R. Hughes, M. Mao, A. R. Jones, J. Burchard, M. J. Marton, K. W. Shannon, S. M. Lefkowitz, M. Ziman, J. M. Schelter, M. R. Meyer, S. Kobayashi, C. Davis, H. Y. Dai, Y. D. D. He, S. B. Stephaniants, G. Cavet, W. L. Walker, A. West, E. Coffey, D. D. Shoemaker, R. Stoughton, A. P. Blanchard, S. H. Friend and P. S. Linsley, *Nat. Biotechnol.*, 2001, **19**, 342–347.
24 A. Pease, D. Solas, E. Sullivan, M. Cronin, C. Holmes and S. Fodor, *Proc. Natl. Acad. Sci. U. S. A.*, 1994, **91**, 5022–5026.
25 M. Pirrung, L. Fallon and G. McGall, *J. Org. Chem.*, 1998, **63**, 241–246.
26 A. R. Pawloski, G. McGall, R. G. Kuimelis, D. Barone, A. Cuppoletti, P. Ciccolella, E. Spence, F. Afroz, P. Bury, C. Chen, C. Chen, D. Pao, M. Le, B. Mcgee, E. Harkins, M. Savage, S. Narasimhan, M. Goldberg, R. Rava and S. P. A. Fodor, *J. Vac. Sci. Technol. B*, 2007, **25**, 2537–2546.
27 O. Srivannavit, M. Gulari, Z. Hua, X. Gao, X. Zhou, A. Hong, T. Zhou and E. Gulari, *Sens. Actuators, B*, 2009, **140**, 473–481.
28 A. Sassolas, B. D. Leca-Bouvier and L. J. Blum, *Chem. Rev.*, 2008, **108**, 109–139.

29 S. Rayner, S. Brignac, R. Bumeister, Y. Belosludtsev, T. Ward, O. Grant, K. O'Brien, G. Evans and H. Garner, *Genome Res.*, 1998, **8**, 741–747.
30 S. Jurczyk, J. Kodra, J. Rozzell, S. Benner and T. Battersby, *Helv. Chim. Acta*, 1998, **81**, 793–811.
31 J. Y. Cheng, H. H. Chen, Y. S. Kao, W. C. Kao and K. Peck, *Nucleic Acids Res.*, 2002, **30**, e69.
32 Y. Y. Huang, P. Castrataro, C. C. Lee and S. R. Quake, *Lab Chip*, 2007, **7**, 24–26.
33 C.-C. Lee, T. M. Snyder and S. R. Quake, *Nucleic Acids Res.*, 2010, **38**, 2514–2521.
34 Z. S. Hua, Y. M. Xia, O. Srivannavit, J. M. Rouillard, X. C. Zhou, X. L. Gao and E. Gulari, *J. Micromech. Microeng.*, 2006, **16**, 1433–1443.
35 M. Moorcroft, W. Meuleman, S. Latham, T. Nicholls, R. Egeland and E. Southern, *Nucleic Acids Res.*, 2005, **33**, e75.
36 K. S. Lam, S. E. Salmon, E. M. Hersh, V. J. Hruby, W. M. Kazmierski and R. J. Knapp, *Nature*, 1991, **354**, 82–84.
37 K. Lam, M. Lebl and V. Krchnak, *Chem. Rev.*, 1997, **97**, 411–448.
38 K. S. Lam, R. Liu, J. Marik and P. R. Kumaresan, *BioMEMS and Biomedical Nanotechnology*, Springer US, 2007, pp. 283–308.
39 X. Yang, S. Bassett, X. Li, B. Luxon, N. Herzog, R. Shope, J. Aronson, T. Prow, J. Leary, R. Kirby, A. Ellington and D. Gorenstein, *Nucleic Acids Res.*, 2002, **30**, e132.
40 A. Ashkin, J. M. Dziedzic, J. E. Bjorkholm and S. Chu, *Opt. Lett.*, 1986, **11**, 288–290.
41 D. G. Grier, *Nature*, 2003, **424**, 810–816.
42 M. MacDonald, G. Spalding and K. Dholakia, *Nature*, 2003, **426**, 421–424.
43 Y. Tanaka, H. Kawada, S. Tsutsui, M. Ishikawa and H. Kitajima, *Opt. Express*, 2009, **17**, 24102–24111.
44 M. Septak, *Nucleic Acids Res.*, 1996, **24**, 3053–3058.
45 *Immobilisation of DNA on Chips II*, ed. Q. Du, C. Wittmann, S. Alegret and F. F. Bier, Birkhuser, Basel, Switzerland, 2006.
46 K. Tanaka, *J. Chem. Soc., Faraday Trans. 1*, 1978, **74**, 1879–1881.
47 R. Hurle and L. Woolf, *J. Chem. Soc., Faraday Trans. 1*, 1982, **78**, 2233–2238.
48 *Low Reynolds Number Hydrodynamics*, ed. J. Happel and H. Brenner, Nijhoff, The Netherlands, 1983.
49 C. Piggee, *Anal. Chem.*, 2009, **81**, 16–19.
50 G. Neale, N. Epstein and W. Nader, *Chem. Eng. Sci.*, 1973, **28**, 1865–1874.
51 T. Wang, unpublished work.
52 Y. Xia and G. Whitesides, *Annu. Rev. Mater. Sci.*, 1998, **28**, 153–184.
53 E. F. Nuwaysir, W. Huang, T. J. Albert, J. Singh, K. Nuwaysir, A. Pitas, T. Richmond, T. Gorski, J. P. Berg, J. Ballin, M. McCormick, J. Norton, T. Pollock, T. Sumwalt, L. Butcher, D. Porter, M. Molla, C. Hall, F. Blattner, M. R. Sussman, R. L. Wallace, F. Cerrina and R. D. Green, *Genome Res.*, 2002, **12**, 1749–1755.
54 S. A. Peyman, A. Iles and N. Pamme, *Lab Chip*, 2009, **9**, 3110–3117.
55 J. Do and C. H. Ahn, *Lab Chip*, 2008, **8**, 542–549.
56 D. S. Kong, P. A. Carr, L. Chen, S. G. Zhang and J. M. Jacobson, *Nucleic Acids Res.*, 2007, **35**, e61.
57 M. C. Huang, H. Ye, Y. K. Kuan, M.-H. Li and J. Y. Ying, *Lab Chip*, 2009, **9**, 276–285.
58 N. Gerry, N. Witowski, J. Day, R. Hammer, G. Barany and F. Barany, *J. Mol. Biol.*, 1999, **292**, 251–262.
59 P. Rothemund, *Nature*, 2006, **440**, 297–302.
60 D. R. Walt, *Chem. Soc. Rev.*, 2010, **39**, 38–50.
61 J. Epstein, J. Ferguson, K. Lee and D. Walt, *J. Am. Chem. Soc.*, 2003, **125**, 13753–13759.